

Femtosecond demagnetization and hot-hole relaxation in ferromagnetic Ga_{1-x}Mn_xAsJ. Wang,^{1,*} Ł. Cywiński,^{2,†} C. Sun,¹ J. Kono,^{1,‡} H. Munekata,³ and L. J. Sham²¹Electrical and Computer Engineering Department, Rice University, Houston, Texas 77005, USA²Department of Physics, University of California, San Diego, La Jolla, California 92093, USA³Imaging Science and Engineering Laboratory, Tokyo Institute of Technology, Yokohama, Kanagawa 226-8503, Japan

(Received 2 April 2008; published 12 June 2008)

We have studied ultrafast photoinduced demagnetization in GaMnAs via two-color time-resolved magneto-optical Kerr spectroscopy. Below band gap midinfrared pump pulses strongly excite the valence band, while near-infrared probe pulses reveal subpicosecond demagnetization that is followed by an ultrafast (~ 1 ps) partial recovery of the Kerr signal. Through comparison with InMnAs, we attribute the signal recovery to an ultrafast energy relaxation of holes. We propose that the dynamical polarization of holes through p - d scattering is the source of the observed probe signal. These results support the physical picture of femtosecond demagnetization proposed earlier for InMnAs, identifying the critical roles of both energy and spin relaxation of hot holes.

DOI: 10.1103/PhysRevB.77.235308

PACS number(s): 78.20.Jq, 42.50.Md, 78.30.Fs

I. INTRODUCTION

Ultrafast studies of collective magnetic phenomena can provide fundamental insights into nonequilibrium processes of correlated spins as well as extend the speed limits of information recording technology.¹ The discovery of photoinduced subpicosecond demagnetization in Ni (Ref. 2) has triggered intense interest in spin dynamics in metallic and insulating magnets.^{3–8} Recently, femtosecond demagnetization, including a total quenching of ferromagnetic order in less than a picosecond, has been observed in InMnAs,⁶ which belongs to the family of (III,Mn)V ferromagnetic semiconductors. We have previously proposed^{6,9,10} that demagnetization in (III,Mn)V materials occurs through sp - d spin scattering between hot holes and localized Mn spins. Here we present a further experimental study of GaMnAs which supports this physical picture.

Carrier-mediated ferromagnetism in (III,Mn)V semiconductors originates¹¹ from the mutual interaction of delocalized hole spins (s) and localized Mn spins (S). The natural division into carrier (hole) and spin (Mn ions) subsystems as well as the simple form of the effective magnetic interaction Hamiltonian between them ($\sim \beta S \cdot s$, where β is the p - d exchange constant) allow for a more transparent treatment of demagnetization than in transition metals.¹² Photoinduced femtosecond demagnetization in InMnAs (Ref. 6) has been well described by the “inverse Overhauser effect,” i.e., the spin-flip scattering between holes and Mn spins enhanced by a high effective temperature of photoexcited carriers.¹⁰ For this model to explain the magnitude of observed demagnetization, the spin-relaxation time of hot holes has to be very short (~ 10 fs) so that each hole can participate in multiple spin-flip scatterings^{6,13} within a relevant time scale (a picosecond). Furthermore, the fact that the fast demagnetization process terminates in less than a picosecond was assumed to be connected with the energy relaxation of excited carriers. However, the ultrafast energy and spin relaxation of strongly excited holes, and its correlation with femtosecond demagnetization, have not been explicitly addressed experimentally until now.

Here we report ultrafast demagnetization and hot-hole relaxation in GaMnAs via two-color time-resolved magneto-

optical Kerr effect (MOKE) spectroscopy. The midinfrared (MIR) pump pulses strongly excite the pre-existing hole population, without creating any photoelectrons in the conduction band. Near-infrared (NIR) probe pulses reveal ultrafast demagnetization followed by a partial recovery of the MOKE signal with a time constant of ~ 1 ps. This “overshoot” behavior, absent in InMnAs, indicates the presence of dichroic bleaching¹⁴ (Pauli blocking of optical transitions) and provides a direct measurement of the energy relaxation of hot holes. The initially highly excited hole population loses its excess energy in less than a picosecond, leading to the rapid termination of the demagnetization process. We argue that the presence of the dichroic bleaching effects in GaMnAs, as opposed to InMnAs, comes from the fact that our probe pulse ($\hbar\omega = 1.6$ eV) is tuned close to the peak of magneto-optical response of GaMnAs,¹⁵ and the relevant transitions involve the states close to the Fermi energy. The population of these states is strongly perturbed by the pump. We discuss in detail the origin of the probe response overshoot and propose that it originates from a transient dynamical polarization of holes, which is a direct consequence of the “inverse Overhauser” mechanism of demagnetization. Finally, the fact that we have not observed any optical orientation effects of holes in GaMnAs excited with a circularly polarized MIR pump shows that photoexcited holes relax their spins on a time scale much shorter than the pulse duration (~ 100 fs), as is required for the theoretical model to work.

II. EXPERIMENTAL RESULTS

The samples studied were a 50 nm Ga_{0.974}Mn_{0.026}As layer on 1 μ m InGaAs and 300 nm GaAs layers and a 25 nm In_{0.87}Mn_{0.13}As layer on a 820 nm GaSb layer. Both were grown by low-temperature molecular-beam epitaxy (LT-MBE) on a semi-insulating GaAs (100) substrate. The Curie temperatures (T_C) were ~ 50 K for the GaMnAs sample and ~ 60 K for the InMnAs sample, and the magnetic easy axes of both samples were parallel to the growth axis due to the tensile strain. In LT-MBE-grown ferromagnetic GaMnAs and InMnAs, there is no clear band gap in optical absorption,

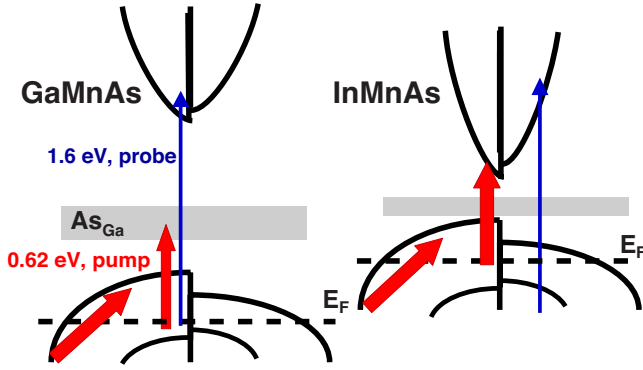


FIG. 1. (Color online) Optical transitions involved in the present experiments on GaMnAs (left) and InMnAs (right) in the ferromagnetic state where the conduction band (CB) and valence band (VB) are spin split. In GaMnAs, below-band-gap pump pulses at 0.62 eV (thick solid arrows) create holes in the VB via transitions from below the Fermi level to the midgap states (e.g., As_{Ga} antisite defect band centered ~ 0.5 eV above the top of the VB) and excite the pre-existing hole population by intervalence band transitions allowed through the relaxation of the k -selection rule. In InMnAs, the photoelectrons in the CB are also created through direct interband transitions. The magnetization changes are probed via Kerr rotation by the reflected, time-delayed pulses at 1.6 eV (thin blue arrows).

which is nonzero for practically all energies.^{16,17} This strong “band tailing” is believed to be due to the defect states present in the gap, such as As_{Ga} antisites and Mn interstitials, and k -selection rule breaking by disorder.^{18,19} As shown in Fig. 1 (left), the MIR pump with 140 fs pulse duration was tuned to 0.62 eV, exciting the valence band in two distinct ways. The first is the generation of more holes by exciting the valence-band electrons from below the Fermi level into the localized midgap states, such as the As_{Ga} antisite level located 0.5 eV above the top of the valence band.²⁰ The second is the inter-valence-band excitation (promoting electrons from below to above the Fermi level in the valence band), allowed by the breaking of the k -selection rule mentioned before. In this process the number of holes does not change, but their temperature is increased. In neither of these processes any conduction-band electrons are created (unlike the case in Refs. 21–25), which allowed us to study ultrafast demagnetization dynamics induced exclusively by the hot holes. The magnetization changes were probed via MOKE rotation⁹ through the reflection of a time-delayed NIR pulse with 140 fs pulse duration. The probe was tuned at 1.6 eV, which gives a static MOKE angle θ_K of 4 mrad. The large pump fluences used, ≈ 8 mJ/cm², ensured that we detected pure demagnetization dynamics, and not the other subtle transient magnetic effects manifested at low-pump fluences, e.g., photoinduced enhancement of magnetization.^{26–29}

Typical time dependence of photoinduced MOKE-angle change, $\Delta\theta_K/\theta_K$, is shown in Fig. 2 for (a) the first 4 ps and for (b) time delays of up to 120 ps. Distinct temporal regimes can be identified: (i) an initial (<200 fs) fast reduction of $\Delta\theta_K/\theta_K$, (ii) a partial recovery of the initial overshoot with a time constant of 1 ps, and (iii) a much slower further decrease in magnetization occurring on the time scale of ~ 100 ps. Process (iii) corresponds to the standard thermal

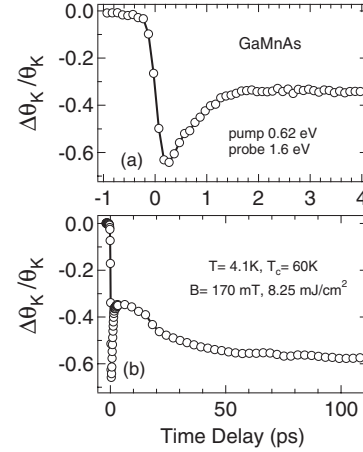


FIG. 2. (a) First 4 ps of $\Delta\theta_K(t)$ for GaMnAs. (b) $\Delta\theta_K(t)$ up to $t=120$ ps. The initial signal is negative (i.e., demagnetization) and very fast, followed by a partial recovery of the MOKE angle with a time constant of ~ 1 ps, and a slow, continuous decrease up to ~ 100 ps.

demagnetization via heat transfer from phonons (spin-lattice scattering).^{6,30} A final recovery toward equilibrium appears much later with a time constant of ~ 2.5 ns (data not shown).

The magnetic-field (B) and temperature (T) dependences of $\Delta\theta_K(t)$ are shown in Figs. 3(a) and 3(b), respectively. In Fig. 3(a) it is seen that the sign of $\Delta\theta_K$ changes when the direction of the field is reversed, and the sign of $\Delta\theta_K/\theta_K$ is always negative (i.e., demagnetization). No $\Delta\theta_K$ is observed at zero field, indicating that without an external field the magnetization direction is not defined between pump pulses (separated by 1 ms) since each pump pulse completely demagnetizes the sample. From this information, using the method described in Ref. 10 we can estimate the effective hole temperature right after photoexcitation, T_h , to be ≥ 700 K for a hole density (p) of $\approx 10^{20}$ cm⁻³. Furthermore, the data in Fig. 3(b) show that $\Delta\theta_K$ decreases drastically as T approaches T_C and is indeed absent above T_C . The overshoot disappears close to T_C , e.g., as seen in the 45 K trace, and $\Delta\theta_K$ is completely absent above T_C . The fact that the magni-

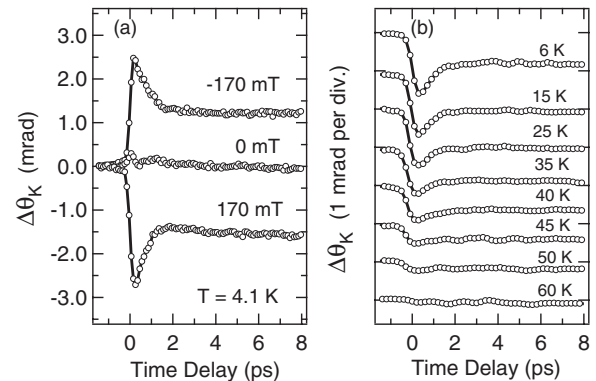


FIG. 3. (a) Magnetic-field dependence of $\Delta\theta_K(t)$. (b) Temperature dependence of $\Delta\theta_K(t)$ from 6 to 60 K. The signal decreases quickly with increasing temperature and is absent above the Curie temperature (~ 50 K).

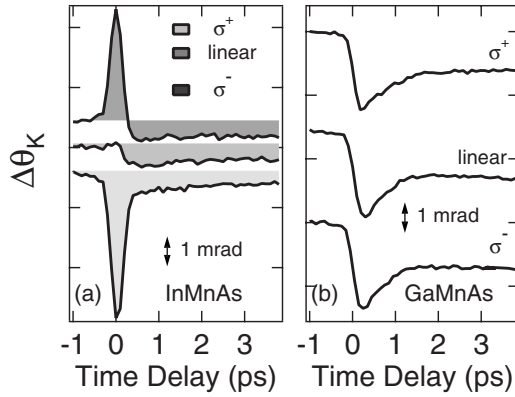


FIG. 4. Photoinduced MOKE dynamics for (a) InMnAs and (b) GaMnAs under pumping with circularly (σ^+ and σ^-) and linearly polarized radiations. The pump and probe photon energies are the same as those in other figures, and the magnetic field is $B > 0$.

tude of the overshoot decays with increasing temperature faster than the “saturated” demagnetization at ~ 1 ps time delay is an important clue to the mechanism behind this feature in the probe response. We discuss it further in Sec. III A.

The MOKE responses of InMnAs and GaMnAs for circularly polarized pump excitation are qualitatively different. Figure 4(a) clearly shows that the initial transients in InMnAs strongly depend on the pump polarization. They disappear within 1 ps, similarly to the transient reflectivity results,⁹ which are dominated by free photoelectrons. From this we infer that these transients are due to the spin-polarized electrons created in the conduction band, and their decay is due to electron trapping by defects, a nonradiative process characteristic for LT-grown materials.⁹ However, in the case of GaMnAs pumped with 0.62 eV light, no free photoelectrons are created. The fact that there is no trace of pump-polarization dependence in the probe response [see Fig. 4(b)] strongly suggests that the optical orientation of photoholes is very quickly destroyed by hole spin relaxation, much shorter than the pulse duration used (~ 140 fs). This is consistent with the theoretical simulations¹⁰ showing that fast (~ 10 fs) spin relaxation of holes is necessary for explaining the observed magnitude of demagnetization.

III. INTERPRETATION AND THEORETICAL MODELING

The magneto-optical response of (III,Mn)V semiconductors below T_C is caused by spin splitting of bands due to the ferromagnetic order, as illustrated in Fig. 1. The optical selection rules arising from spin-orbit coupling in the valence band of III-V semiconductors then lead to different optical responses to the two circular polarizations of light σ_{\pm} . Within the *sp-d* model of ferromagnetism,^{11,33} the band splitting Δ is proportional to the average localized spin. In the static (equilibrium) case, only this band splitting in the ground state is probed, and the MOKE response is proportional to the macroscopic magnetization of the Mn spins. In time-resolved measurements with *strong photoexcitation* discussed here, holes excited by the pump can influence the magneto-optical response in other distinctly different ways.

Besides the splitting of bands, the MOKE signal is also directly influenced by state filling,¹⁴ provided that the probe light couples to the states whose occupation was strongly modified by the pump. Therefore, a selective pump-probe relaxation dynamics of hot carriers. For example, the previously discussed pump-polarization dependent transients in InMnAs arise from the creation of spin-polarized photoelectrons in the conduction band, leading to the bleaching of transitions induced by the part of the probe beam copolarized with the pump.

One of our main observations for GaMnAs is the initial prominent overshoot behavior, which is not seen in InMnAs.⁶ This is clearly visible in the $\Delta\theta_K(t)$ traces for a linearly polarized pump (center) in Figs. 4(a) and 4(b). In InMnAs the transitions away from the Γ point (originating below the quasi-Fermi level of strongly excited valence-band electrons) contribute to the optical response at 1.6 eV. Due to the very small effective mass in the conduction band of InMnAs, the thermalized photoelectrons can still bleach the probe transitions, but it is plausible that most of the initial states in the valence-band contributing to the probe response are far away from those affected by the pump excitation, as illustrated in Fig. 1 (right). Consequently, apart from the electron-related transient, the MOKE signal in InMnAs arises from the changes in average Mn polarization.⁶ On the other hand, in the case of GaMnAs (see Fig. 1, left), the probe frequency was tuned near the peak of the static MOKE spectra of GaMnAs.^{15,31,32} The transitions responsible for this peak were most commonly assumed to involve final states in the conduction band,^{18,33} but in recent experiments other possibilities were discussed. Final states in the dispersionless level close to the bottom of the conduction band were proposed.³² It has also been argued that most of the magneto-optical spectrum of GaMnAs at ~ 1.6 eV is dominated by transitions involving the intragap states.^{15,34} Our findings support these interpretations, as our calculations of magneto-optical spectra of GaMnAs using the $\mathbf{k}\cdot\mathbf{p}$ band model³³ agree qualitatively with the published measurements^{15,31} only for a very low hole concentration, $p \sim 10^{19}$ cm⁻³, which disagrees with the critical temperatures of most of the measured samples. In any case, the probe couples to electronic transitions for which the initial states are in the valence band, close to the Fermi level. These are exactly the states whose population is strongly disturbed by the pump. Taking into account that the holes relax their spin very quickly, we expect prominent, pump-polarization-independent dichroic bleaching in GaMnAs. This expectation is confirmed by the results shown in Fig. 4(b).

A. Sources of dichroic bleaching

There are two possible sources for the dichroic bleaching signal observed in GaMnAs. The first is a simple blocking of transitions by photoholes added to the valence band, which diminishes the absorption α_{\pm} for both circular polarizations. Although θ_K is a complicated function of the optical constants of the material (especially in the relevant case of reflection from a layered material), it is generally proportional

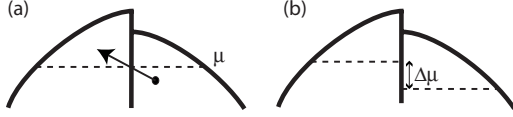


FIG. 5. Illustration of the spin bottleneck effect for a (III,Mn)V semiconductor. (a) Hole spin-flip scattering event which leads to demagnetization of the localized spins (this is the dominant scattering event when holes are hot and Mn are fully polarized), with μ being the chemical potential. The band is spin split by exchange interaction with the localized spins. (b) When the spin-relaxation time of holes is finite, such scattering leads to the dynamical polarization of holes, parametrized by the spin splitting $\Delta\mu$ of the quasi-chemical potentials.

to $\alpha_+ - \alpha_-$. When the two absorption coefficients are down-scaled by the same factor, the MOKE signal is suppressed.

The second source of dichroic bleaching is the dynamical polarization of holes created in the process of demagnetization. The following scenario assumes that the Kerr response of the probe corresponds not to the average band splitting (proportional to the average Mn spin) but to the average polarization of hot holes in the valence band.

When the holes are very hot, the enhanced rate of p - d scattering with the Mn spins leads to the transfer of angular momentum from the localized spins to the holes. Unless the hole spin relaxation is instantaneous, the nonequilibrium (dynamical) spin polarization of holes is created, i.e., their average spin ceases to be proportional to the average Mn spin. This is described by the equation for the dynamics of the average hole spin $\langle s^z(t) \rangle$,

$$\frac{d}{dt} \langle s^z(t) \rangle = -\frac{n_i}{p} \frac{d}{dt} \langle S^z(t) \rangle - \frac{\langle s^z(t) \rangle - s_0(t)}{\tau_{sr}}, \quad (1)$$

in which n_i and p are the densities of Mn and holes, respectively, $\langle S^z(t) \rangle$ is the average Mn spin, s_0 is the instantaneous equilibrium value of the average hole spin (determined by T_h and the band splitting $\Delta \sim \langle S^z(t) \rangle$), and τ_{sr} is the hole spin-relaxation time. The first term on the right-hand side is due to the p - d spin-flip scattering, and it is responsible for the dynamical polarization of holes. If the second term was not efficient enough (if τ_{sr} was too long), the holes would get dynamically polarized to such a degree that there would be no more holes with the spin suitable for p - d scattering with the Mn spins. Then the demagnetization process would cease.

For antiferromagnetic coupling between the Mn spins and valence-band electrons³⁵ ($\beta < 0$ in the standard notation for dilute magnetic semiconductors), spin-flip scattering between hot holes and Mn spins leads to a *decrease* in the hole spin polarization, as shown in the schematic illustration in Fig. 5. Therefore, assuming a finite hole spin-relaxation time τ_{sr} , the net spin in the valence band during the transient dynamics is actually *lower* than the equilibrium value corresponding to the instantaneous Mn magnetization. Let us mention here the existence of a competing process, in which the hot holes are simply relaxing their average spin toward the instantaneous equilibrium value s_0 [the second term on the left-hand side of Eq. (1)]. For values of parameters used

in our calculations this enhances the effect due to the dynamical polarization.

An important observation is that the assumption of $\theta_K(t) \propto \langle s^z(t) \rangle$ leads to a natural explanation of the temperature dependence of the overshoot feature in Fig. 3(b). At temperatures slightly below T_C , the initial Mn polarization is very small. During the demagnetization, the amount of angular momentum transferred from Mn spins to holes is much smaller than at low T , and the spin relaxation of holes can effectively suppress their dynamical polarization ($\Delta\mu \approx 0$ in Fig. 5). The changes in $\langle s^z(t) \rangle$ due to relaxation toward $s_0(T_h, \Delta)$ are also suppressed at small values of Δ . Thus, the disappearance of the overshoot before the vanishing of the real demagnetization can be qualitatively explained in this scenario. It is not so if we assume that the overshoot simply comes from strong bleaching of all the optical transitions, in which case it should remain visible at all $T < T_C$.

B. Calculation of Mn and hole spin dynamics

In order to quantitatively model the transient dynamics of the hole population, we solve the equation for dynamics of the average Mn spin $\langle S^z(t) \rangle$,

$$\frac{d}{dt} \langle S^z(t) \rangle = \sum_{m=-5/2 \dots 5/2} m \frac{d}{dt} \rho_m(t), \quad (2)$$

where the time dependence of the diagonal elements of the localized spin-density matrix ρ_m is given by the rate equations

$$\frac{d}{dt} \rho_m = -(W_{m-1,m} + W_{m+1,m}) \rho_m + W_{m,m+1} \rho_{m+1} + W_{m,m-1} \rho_{m-1}. \quad (3)$$

The transition rates $W_{m,m\pm 1}$ depend on the distribution of holes (their temperature and polarization). The full expressions and details of their calculation are given in Ref. 10. Here we only need to know that the spin-flip rates W are proportional to the temperature of holes T_h . The equation for the dynamics of $\langle S^z(t) \rangle$ is coupled with Eq. (1) for the dynamics of the average hole spin. Finally, the temperature of holes after the end of the pulse is assumed to decay as $T_h(t) \sim \exp(-t/\tau_E)$ with energy relaxation time τ_E . The fact that T_h decays here toward zero instead of the final hole temperature (which is about 50–100 K) is irrelevant for the dynamics during the first couple of picoseconds—after T_h drops to about 100 K the demagnetization becomes very slow and it does not matter for our purposes.

We have performed calculations using the effective Hamiltonian model,^{33,37} in which the mean-field spin splitting is added to the six band Luttinger model. We have used the spin-relaxation time $\tau_{sr} = 10$ fs and adjusted the energy relaxation time $\tau_E = 1$ ps to fit the observations. Figure 6 shows our calculated time dependence of Mn and hole spin polarizations after excitation. The Mn spins demagnetize by $\sim 20\%$, in qualitative agreement with the experimental data in Fig. 2, and the time scale of the dynamical process (demagnetization of Mn and dynamical polarization of holes) is limited by the energy relaxation time τ_E —as T_h decreases, the

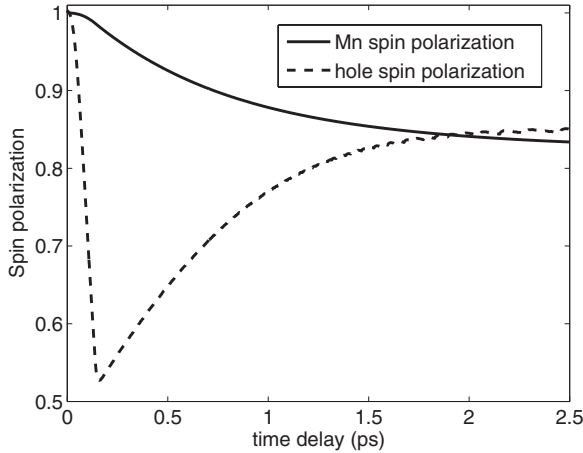


FIG. 6. Simulation of the time dependence of the Mn spin polarization (the macroscopic magnetization) and the hole spin polarization after excitation with 140-fs-long pulse of light. The influence of the pulse is modeled as a rise of hole temperature T_h from 4 to 1000 K right after the end of the pulse. Other parameters are total $p=10^{20}$ cm $^{-3}$, energy relaxation time of holes $\tau_E=1$ ps, their spin-relaxation time $\tau_{sr}=10$ fs, and p - d exchange constant $N_0\beta=-1$ eV (with N_0 being the cation density), which for Mn concentration $x=0.26$ leads to the initial spin splitting of the valence band of 70 meV.

phase space available for hole scattering diminishes, and the efficiency of hole-Mn spin-flip drops. The depolarization of holes exhibits a prominent overshoot, suggestively similar to the observed MOKE signal. Thus, under our assumption that $\theta_K \propto \langle s^z \rangle$ in GaMnAs, the dynamical polarization of holes can explain the observed temporal profile of the probe response.

C. Energy relaxation of holes

The distinct overshoot behavior in GaMnAs, absent in InMnAs, provides a clue for understanding the ultrafast relaxation dynamics of holes in (III,Mn)V semiconductors. We attribute the partial recovery of the MOKE signal with a time constant of ~ 1 ps to the energy relaxation of highly excited holes. It is important to note that much less is known experimentally about the ultrafast dynamics of holes than that of electrons, especially in a regime of strong excitation. In our case $\sim 10^{20}$ cm $^{-3}$ hot holes are distributed in a very wide energy region (comparable to $k_B T_h \approx 0.1$ eV, with an effective temperature T_h of $\approx 10^3$ K after thermalization). This regime remains largely unexplored by experiments. Let us reiterate that our τ_E is the characteristic time scale of the *initial* large energy loss of the very hot holes, i.e., the decay

of their temperature from about 10^3 to $\sim 10^2$ K, with the latter value already corresponding to a slow demagnetization dynamics (time scale of tens of picoseconds). Theoretical calculations of energy-loss rates for high-energy holes suggest that such a highly excited population will lose a significant part of its energy through phonon emission during the first picosecond,³⁸ in agreement with our measurements. Moreover, the picosecond energy relaxation of holes explains the rapid termination of the demagnetization process very well.

IV. CONCLUSIONS

We have observed photoinduced subpicosecond demagnetization in GaMnAs. Because of the disordered nature of GaMnAs, the midinfrared pump strongly excites the valence band. This leads to demagnetization of the Mn spins, which proceeds as long as the holes are hot. We propose that the initial overshoot in the drop of the probe Kerr signal is related to a strong excitation of holes near the Fermi level, which bleaches the magneto-optical response of the probe. A possible scenario is the appearance of transient dynamical polarization of hot holes (due to enhanced spin-flip scattering with Mn spins). Under assumption that the probe signal, at frequency of the transitions originating close to the Fermi level, is dominated by the average spin polarization in the valence band (and not the average Mn polarization), such a dynamical polarization leads to an overshoot in qualitative agreement with the observation. However, more work on understanding the equilibrium and nonequilibrium magneto-optical properties of GaMnAs is necessary in order to verify this interesting scenario. The subsequent subpicosecond recovery of Kerr rotation is interpreted as a signature of fast energy relaxation of holes. As expected, ultrafast demagnetization stops after this relaxation time. Hole spin-relaxation time much shorter than the pulse width is inferred from the polarization dependence, consistent with our previously proposed theoretical model.

ACKNOWLEDGMENTS

This work was supported by DARPA (Grant No. MDA972-00-1-0034), NSF (Grants No. DMR-0134058, No. DMR-0325474, No. DMR-0325599, and No. OISE-0530220), and ONR (Grant No. N000140410657). In addition, this work was supported in part by Grant-in-Aid for Scientific Research from JSPS (No. 17206002) and MEXT (No. 19048020).

*Present address: Lawrence Berkeley National Laboratory, Berkeley, CA, USA; jwang5@lbl.gov

†Present address: Condensed Matter Theory Center, Department of Physics, University of Maryland, College Park, MD, USA; lcyw@umd.edu

‡Corresponding author; kono@rice.edu

¹C. D. Stanciu, F. Hansteen, A. V. Kimel, A. Kirilyuk, A. Tsukamoto, A. Itoh, and Th. Rasing, Phys. Rev. Lett. **99**, 047601 (2007).

²E. Beaurepaire, J. C. Merle, A. Daunois, and J.-Y. Bigot, Phys.

- Rev. Lett. **76**, 4250 (1996).
- ³G. Zhang, W. Hübner, E. Beaurepaire, and J.-Y. Bigot, *Top. Appl. Phys.* **83**, 245 (2002).
- ⁴B. Koopmans, *Top. Appl. Phys.* **87**, 253 (2003).
- ⁵A. V. Kimel, R. V. Pisarev, J. Hohlfeld, and T. Rasing, *Phys. Rev. Lett.* **89**, 287401 (2002).
- ⁶J. Wang, C. Sun, J. Kono, A. Oiwa, H. Munekata, Ł. Cywiński, and L. J. Sham, *Phys. Rev. Lett.* **95**, 167401 (2005).
- ⁷A. V. Kimel, A. Kirilyuk, A. Tsvetkov, R. V. Pisarev, and T. Rasing, *Nature (London)* **429**, 850 (2004).
- ⁸A. V. Kimel, A. Kirilyuk, P. A. Usachev, R. V. Pisarev, A. M. Balbashov, and T. Rasing, *Nature (London)* **435**, 655 (2005).
- ⁹J. Wang, C. Sun, Y. Hashimoto, J. Kono, G. A. Khodaparast, Ł. Cywiński, L. J. Sham, G. D. Sanders, C. J. Stanton, and H. Munekata, *J. Phys.: Condens. Matter* **18**, R501 (2006).
- ¹⁰Ł. Cywiński and L. J. Sham, *Phys. Rev. B* **76**, 045205 (2007).
- ¹¹T. Dietl, H. Ohno, F. Matsukura, J. Cibert, and D. Ferrand, *Science* **287**, 1019 (2000).
- ¹²B. Koopmans, J. J. M. Ruigrok, F. Dalla Longa, and W. J. M. de Jonge, *Phys. Rev. Lett.* **95**, 267207 (2005).
- ¹³A. V. Akimov, A. V. Scherbakov, D. R. Yakovlev, I. A. Merkulov, M. Bayer, A. Waag, and L. W. Molenkamp, *Phys. Rev. B* **73**, 165328 (2006).
- ¹⁴B. Koopmans, M. van Kampen, J. T. Kohlhepp, and W. J. M. de Jonge, *Phys. Rev. Lett.* **85**, 844 (2000).
- ¹⁵K. Ando, H. Saito, K. C. Agarwal, M. C. Debnath, and V. Zayets, *Phys. Rev. Lett.* **100**, 067204 (2008).
- ¹⁶E. J. Singley, K. S. Burch, R. Kawakami, J. Stephens, D. D. Awschalom, and D. N. Basov, *Phys. Rev. B* **68**, 165204 (2003).
- ¹⁷K. Hirakawa, A. Oiwa, and H. Munekata, *Physica E (Amsterdam)* **10**, 215 (2001).
- ¹⁸J. Szczytko, W. Bardyszewski, and A. Twardowski, *Phys. Rev. B* **64**, 075306 (2001).
- ¹⁹K. Dziatkowski, Ł. Cywiński, W. Bardyszewski, A. Twardowski, H. Saito, and K. Ando, *Phys. Rev. B* **73**, 235340 (2006).
- ²⁰S. Lodha, D. B. Janes, and N. Chen, *J. Appl. Phys.* **93**, 2772 (2003).
- ²¹J. Wang, Y. Hashimoto, J. Kono, A. Oiwa, H. Munekata, G. D. Sanders, and C. J. Stanton, *Phys. Rev. B* **72**, 153311 (2005).
- ²²G. D. Sanders, C. J. Stanton, J. Wang, J. Kono, A. Oiwa, and H. Munekata, *Phys. Rev. B* **72**, 245302 (2005).
- ²³A. Oiwa, Y. Mitsumori, R. Moriya, T. Slupinski, and H. Munekata, *Phys. Rev. Lett.* **88**, 137202 (2002).
- ²⁴Y. Mitsumori, A. Oiwa, T. Slupinski, H. Maruki, Y. Kashimura, F. Minami, and H. Munekata, *Phys. Rev. B* **69**, 033203 (2004).
- ²⁵A. V. Kimel, G. V. Astakhov, G. M. Schott, A. Kirilyuk, D. R. Yakovlev, G. Karczewski, W. Ossau, G. Schmidt, L. W. Molenkamp, and T. Rasing, *Phys. Rev. Lett.* **92**, 237203 (2004).
- ²⁶J. Wang, I. Cotoros, K. M. Dani, X. Liu, J. K. Furdyna, and D. S. Chemla, *Phys. Rev. Lett.* **98**, 217401 (2007).
- ²⁷J. Wang, I. Cotoros, K. M. Dani, D. S. Chemla, X. Liu, and J. K. Furdyna, *Proc. SPIE* **6892**, 68920Q (2008).
- ²⁸J. Wang *et al.*, arXiv:0804.3456 (unpublished).
- ²⁹J. Chovan, E. G. Kavousanaki, and I. E. Perakis, *Phys. Rev. Lett.* **96**, 057402 (2006).
- ³⁰E. Kojima, R. Shimano, Y. Hashimoto, S. Katsumoto, Y. Iye, and M. Kuwata-Gonokami, *Phys. Rev. B* **68**, 193203 (2003).
- ³¹B. Beschoten, P. A. Crowell, I. Malajovich, D. D. Awschalom, F. Matsukura, A. Shen, and H. Ohno, *Phys. Rev. Lett.* **83**, 3073 (1999).
- ³²R. Lang, A. Winter, H. Pascher, H. Krenn, X. Liu, and J. K. Furdyna, *Phys. Rev. B* **72**, 024430 (2005).
- ³³T. Dietl, H. Ohno, and F. Matsukura, *Phys. Rev. B* **63**, 195205 (2001).
- ³⁴S. Picozzi, A. Continenza, M. Kim, and A. J. Freeman, *Phys. Rev. B* **73**, 235207 (2006).
- ³⁵Although β is often referred to as “the hole exchange constant,” in reality it is the exchange constant in the Hamiltonian of the Mn spin valence *electron* (ve) interaction, given by $H_{p-d} = -\beta \mathbf{S}_{\text{Mn}} \cdot \mathbf{s}_{\text{ve}}$; see, e.g., Ref. 36.
- ³⁶P. Kacman, *Semicond. Sci. Technol.* **16**, R25 (2001).
- ³⁷T. Jungwirth, J. Sinova, J. Mašek, J. Kučera, and A. H. MacDonald, *Rev. Mod. Phys.* **78**, 809 (2006).
- ³⁸M. Woerner and T. Elsaesser, *Phys. Rev. B* **51**, 17490 (1995).